A New Electromagnetic Valve Actuator

W. S. Chang[‡], T. A. Parlikar[‡], M. D. Seeman[‡], D. J. Perreault[†], J. G. Kassakian[*], and T. A. Keim[†]
[*]*Fellow, IEEE* [†]*Member, IEEE* [‡]*Student Member, IEEE*
Massachusetts Institute of Technology
Laboratory for Electronic and Electromagnetic Systems
77 Massachusetts Avenue
Cambridge, MA 02139
Telephone: (617) 452-1976
Fax: (617) 258-6774
Email: tkeim@mit.edu

***Abstract*—In conventional internal combustion (IC) engines, engine valve displacements are fixed relative to crankshaft position. If these valves are actuated as a variable function of crankshaft angle, significant improvements in fuel economy can be achieved. Existing electromagnetically actuated variable-valve-timing (VVT) systems characteristically use springs to provide the large inertial power to move the engine valves. However, the large spring forces generated when the valve is being closed or opened make it difficult to hold the valve without using a normal-force electromagnetic actuator. With normal-force electromagnetic actuators, it is difficult for the valve to engage its seat at a low velocity. Furthermore, from a control systems perspective, these unidirectional normal-force actuators pose difficult design challenges when compared to bi-directional shear-force actuators, as the former have nonuniform force constants. In this paper, we propose a novel electromagnetic valve drive (EMVD) system, and discuss the design and construction of the experimental apparatus, power electronics and controllers for the EMVD. This EMVD comprises an electric motor that is coupled to an engine valve-spring system with a nonlinear mechanical transformer. Simulation results show significant advantages of this EMVD over previously designed actuation systems.**

***Index Terms*— Actuator, Electromagnetic, Engine, Nonlinear, Mechanical, Spring, Transformer, Valve.**

I. Introduction

AUTOMOTIVE electrical systems today are moving towards higher power requirements. Due to the resulting increase in electrical load, the automotive industry established a new 42V voltage standard that will eventually replace the current 14V system [1], [2]. The introduction of this standard, coupled with recent advances in power electronics, sensors and microprocessors, has led to several innovations in automotive systems. Many of these innovations significantly increase fuel economy, and some involve the replacement of automotive mechanical systems with electrical systems [3]. Of particular relevance, the new voltage standard has made the electrification of internal combustion (IC) engine valves a technically and economically viable innovation.

In conventional IC engines, engine valve displacements are fixed relative to the crankshaft position. The valves are actuated with cams that are located on a belt-driven camshaft, and the shape of these cams is determined by considering a tradeoff between engine speed, power, and torque requirements, as well as vehicle fuel consumption. This optimization results in an engine that is highly efficient only at certain operating conditions [4], [5]. Instead, if the engine valves are actuated as a variable function of crankshaft angle, significant improvements in fuel economy - up to 20% - can be achieved [6]. In addition, improvements in torque, output power and emissions are achieved.

Internal combustion engines in which both the duration (how long each valve is opened or closed) and the phase (how each valve profile is shifted with respect to some nominal valve profile) of the valves can be controlled are said to have variable valve timing (VVT) [7]. VVT can be achieved using either mechanical or electromechanical actuation systems. In this paper, the focus is on an electromechanical actuation system. With VVT alone, a 10% improvement in fuel economy can be achieved [6]. Furthermore, if the lift (how much each valve is opened) of the valves is controlled, another 10% improvement can be gained.

Currently, the most advanced VVT system is an electromagnetic engine valve actuation system that includes a valve-spring system coupled to two electromagnetic normal-force actuators. Although these actuators are well-suited to holding the engine valve open or closed, there are some fundamental design challenges posed by this actuation system, especially in the area of controller design.

In order to solve the significant design challenges associated with electromagnetic normal-force actuated VVT systems, we have proposed an electromechanical valve drive (EMVD) incorporating a nonlinear mechanical transformer [4], [8]. In simula-

tions, the proposed EMVD allows for small holding and driving currents, and small seating velocity (velocity at which the valve engages its seat). The peak and average power for the EMVD are also reasonable. An experimental apparatus to test the concept of the EMVD has been designed and constructed.

In this paper, we describe some previously designed VVT systems and then focus on the proposed EMVD. This EMVD has several important implications for the design of its power electronics and controllers. We will discuss these implications and describe the design and construction of an experimental apparatus to validate the concept of this EMVD.

This document is organized as follows: in Section II, we summarize previous work in the area of electromagnetic valve actuators, and motivate the need for the proposed EMVD. In Section III, the proposed EMVD is described in detail. Section IV describes the design and simulation of controllers for the EMVD. Section V describes the experimental apparatus and the associated design issues. Section VI briefly discusses the electrical/electronics implications of the proposed EMVD design. Section VII concludes this paper.

II. Background and Motivation

An IC engine valve's kinematics profiles (such as valve position versus time, valve speed versus time, and so on) are of fixed shape and are timed relative to the engine crankshaft position. From a control systems perspective, we say the engine valves are not controllable. If instead, we could independently control the duration, phase and lift of the valves, a marked improvement in emissions, efficiency, maximum power, and fuel economy would be seen. The engine's mechanical design, although simple, compromises the efficiency and maximum power of the engine [7]. However, any variable valve actuation system must be able to offer a variable valve profiles without compromising the essential characteristics of a conventional IC engine valve profile, which are described next.

Let us examine the kinematics variables for a conventional IC engine valve, as shown in Fig. 1. In the figure, the valve stroke is defined as the displacement of the valve from fully-open to fully-closed positions [6]. Valve transition time is defined as the time taken for the valve to go from one end of its stroke to the other. The inertial power profile shown in Fig. 1 is obtained as the product of inertial force and valve velocity, and has an instantaneous peak value on the order of 2–3kW for each valve in a typical engine. The average power losses associated with driving the engine valves is approximately 3kW for 16 valves in a 2.0L, 4 cylinder engine at 6000rpm engine speed and wide open throttle.

There are a few important points to make about Fig. 1. First, although the valve inertial power is very large, it is also regenerative – after an initial input of inertial power, this inertial power

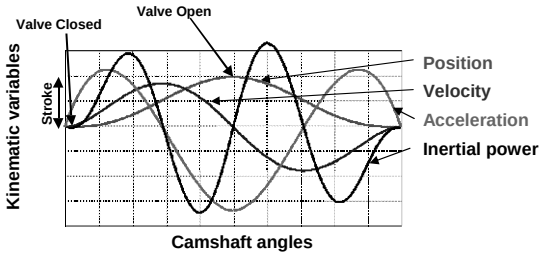

Fig. 1. Conventional Valve Train Profiles.

is regenerated continuously. A spring is used to store the initial required energy and then the energy is transferred cyclically to the engine valve and cam. To be a competitive technology, any variable valve actuation system must be able to provide this large inertial power economically [4], [8]. Second, the seating velocity of the valve is small (less than 3cm/s at 600rpm engine speed, and less than 30cm/s at 6000rpm engine speed), which allows for the so-called soft landing of the valve. In order to prevent excessive wear of engine valves, any variable valve actuation system should allow for the soft landing of the valve. Third, an engine valve's kinematics profiles are inherently smooth. From a mechanical design perspective, discontinuities in valve kinematics profiles can generate undesirable impacts/losses and acoustical noise.

With an electromagnetically-driven variable valve timing system (VVT), one can independently control the phase and duration of the engine valve profiles, and carry out variable engine displacement (where certain cylinders in the engine are deactivated). In these VVT systems, the valve can be held in the open or closed positions for a variable time period (called the holding time), and it transitions from one end of the stroke to the other in the transition time. Prototype electromagnetically-actuated VVT systems have been proposed by several companies in the automotive industry, the first being proposed and patented by FEV Motorentechnik [9], [10]. Other companies that have worked on this technology include BMW [11], [12], GM [13], Renault [14], [15], Siemens [5], [16], and Aura [17].

Most electromagnetically-driven VVT systems have emulated one of the main characteristics of conventional IC valve profiles – that of regenerative inertial power. At the heart of these actuators is a valve-spring system, where an engine valve is coupled to two springs (with the same spring constant) as shown in Fig. 2. The equilibrium position for this mass-spring system is in the middle of the valve stroke. Such a system has an inherent natural frequency (ω_n), mass (m), effective spring constant (k), and damping ratio (ζ). Assuming there was no damping, an initial displacement of the valve in the direction of either spring would result in sustained oscillations of the valve at the system's natural frequency ($\omega_n = \sqrt{\frac{k}{m}}$).

In the ideal frictionless case, considering only the dynamics

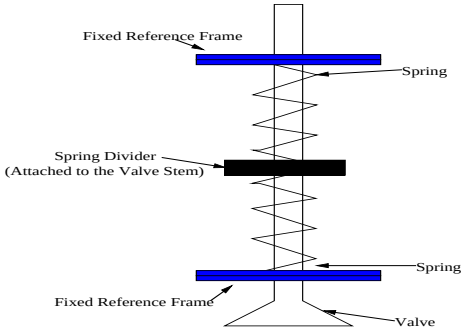

Fig. 2. An Engine Valve-Spring System.

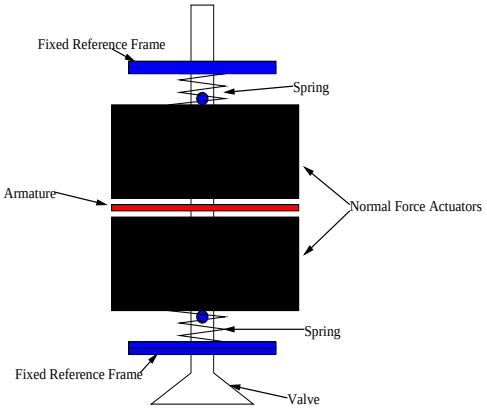

Fig. 3. A Normal-Force Actuated Valve-Spring System.

of the valve, the electromechanical actuator for the valve-spring system only has to be able to hold the valve at either end of its stroke. In reality, due to gas forces in the engine, especially on the exhaust valves, additional work is required to reject the gas force disturbance. In addition, as the spring forces increase linearly with valve displacement, these forces are largest at the ends of the stroke, making it difficult to hold the valve in the open or closed position without using a large holding force, and thus a lot of electrical power [4].

The most popular method of controlling the valve-spring system is to use two solenoids: one to hold the valve open and one to hold the valve closed [9], [10]. Fig. 3 shows a normal-force actuated valve-spring system [8]. Each electromagnet exerts a unidirectional normal force, and thus, the system employs two normal force actuators. The force exerted by these actuators is proportional to the square of the current input, but decreases as a function of the air gap between the actuator and the armature. Hence, these actuators have a nonuniform force constant. For a fixed level of current, the solenoids exert large forces when the valve is at their end of the stroke, but small forces when the valve is at the far end of the stroke. For example, when the valve is at the upper end of its stroke, the upward-acting solenoid can produce a large force with a relatively small current. However, when the valve is at the lower end of its stroke, a large upward force requires a very large current in the upward-acting solenoid.

Let us take a closer look at the free-flight dynamics for a normal-force actuated valve-spring system without friction, and gravitational and gas forces, as shown in Fig. 4 [8]. The kinematics profiles in Fig. 4 can be easily explained. Suppose the valve is held closed by turning on the lower normal-force actuator. Ideally, if the valve were released, it would be accelerated by the springs past the equilibrium position of the system to its open position, where it would naturally stop. In reality, friction, and gravitational and gas forces prevent the valve from reaching the open position, and thus, near the open position, the second normal-force actuator is turned on, and the valve is pulled into its open position.

In the idealized motion described above, the springs play a large role because they provide the large inertial power to accelerate the valve at the beginning of its stroke, and then to absorb the inertial power to decelerate the valve at the ends of its stroke. As was the case in conventional IC engine valves, this inertial power is regenerative because energy is stored in the springs instead of being dissipated. In addition, due to the electromagnet-actuators' nonuniform force-displacement characteristics, the current required to hold the valve open or closed (holding current) is small [8].

One of the other desirable characteristics for VVT systems is that of soft landing for the valves: the valves should reach either end of the stroke with very small velocity and acceleration. However, there are substantial control challenges to achieving soft landing with normal-force actuators. First, since the normal-force actuators are unidirectional, it is very difficult to decelerate the valve as it approaches an end of its stroke. To arrive exactly at the end of the stroke with exactly zero velocity (defined as perfect soft landing), the receiving-end actuator must do exactly as much work as was done against friction and gas force over the entire transition. If the actuator does not do this much work, the valve will stop before the end of the stroke, and will be driven away again by the spring. If the actuator does any more than the exactly correct work, the valve arrives at the end of the stroke with non-zero velocity, and impacts the valve seat.

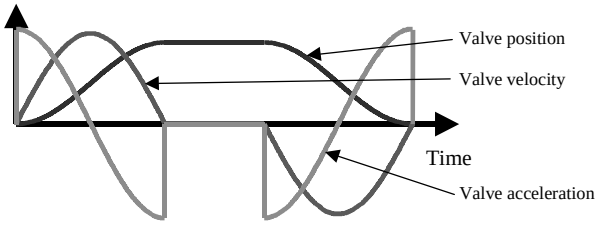

Fig. 4. Kinematics Profiles for a Normal-Force Actuated Valve-Spring System.

A second control challenge is that the electromagnetic actuators have a nonuniform force constant, making it difficult to apply enough force to the valve when it is close to the equilibrium point of the system. Thus, it is difficult to counteract the effects of the gas force disturbance on the system.

In the idealized free-flight valve-spring dynamics, as shown in Fig. 4, we can observe that the acceleration curve has discontinuities at both the end and beginning of the stroke. These discontinuities assume the instantaneous release of the valve at the beginning of the stroke and the instantaneous capture of the valve at the end of the stroke. These instantaneous actions require step changes in force. A true step force would create shock waves in the system and produce audible noise. To reduce this noise, it is possible to release the valves more slowly, but this lengthens transition time and increases the work which the capturing actuator must do.

A possible solution to the control challenges in the normal-force actuated valve-spring system is to attempt to use a bi-directional shear force actuator (see [13], [18], [19]) to control the valve-spring system. An example of such an actuator is a rotary electric motor. Such actuators have a uniform force constants and can exert bi-directional forces. Fig. 5 shows the results from a simulation of a feedback-controlled valve-spring system with a rotary electric motor as the actuator [8]. As was the case before, the equilibrium position of the system is at the midpoint of the stroke. The reference input for this simulation was a smooth valve profile.

As expected, with active control and a bi-directional shear-force actuator, the effect of gas force is reduced by the controller, while the valve kinematics profiles are smooth - thereby eliminating the soft-landing problem inherent in normal-force actuated valve-spring systems. However, there are problems with this VVT system. First, the holding current is very high because the spring forces at the ends of the stroke are large. Second, the required driving current to follow smooth valve kinematics profiles is also large. Thus, the corresponding power loss of this VVT system is too large to be economically feasible [8].

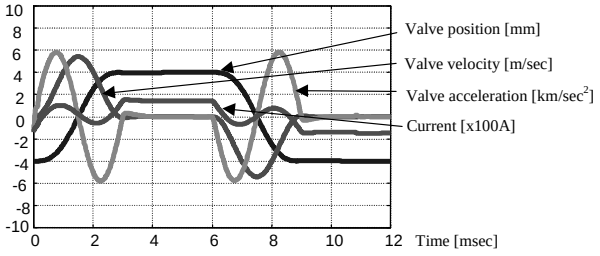

Fig. 5. Simulation of a Feedback-Controlled Shear-Force Actuated Engine Valve-Spring System.

III. The Proposed EMVD

In order to solve the problems associated with the previously discussed VVT systems, we have proposed an EMVD incorporating a nonlinear mechanical transformer [8]. This EMVD comprises an electric motor that is coupled to a valve spring system with a nonlinear mechanical transformer (NTF). Fig. 6 shows a schematic of this EMVD and Fig. 7 shows a desirable nonlinear mechanical transformer characteristic between the z and θ domains [8].

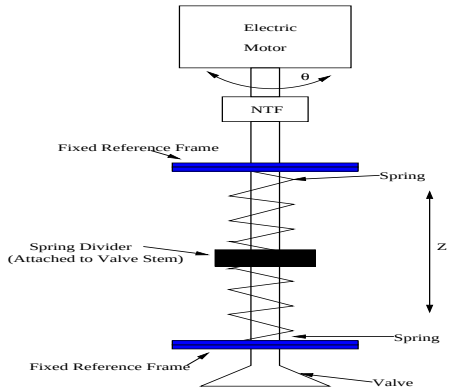

Fig. 6. A Schematic of the Proposed EMVD.

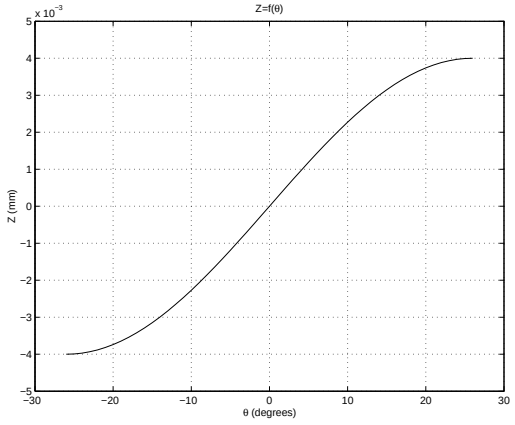

Fig. 7. A Desirable Characteristic for the NTF.

In the proposed EMVD, the electric motor acts as a uniform force constant actuator, giving an excellent control handle over valve position in the z domain. Using well-known active control techniques, small seating velocities, small position and velocity errors, and smooth kinematics variables can be achieved. In addition, the characteristic of the NTF can be designed such that the holding and driving currents in the system are reduced.

Since θ is a function of z and vice-versa, it is easy to show that the following relations hold between θ and z [4], [8]:

$$z = f(\theta) \Longrightarrow \theta = f^{-1}(z) \tag{1}$$

$$\frac{d\theta}{dt} = \frac{d\theta}{dz} \cdot \frac{dz}{dt} \tag{2}$$

$$\frac{d^2\theta}{dt^2} = \frac{d^2\theta}{dz^2} \cdot (\frac{dz}{dt})^2 + \frac{d\theta}{dz} \cdot \frac{d^2z}{dt^2} \tag{3}$$

The NTF provides a very desirable coupling between the z and θ domains. By equating the energy in the z and θ domains and using the NTF characteristic, the following relation results:

$$\tau_\theta = \frac{dz}{d\theta} \cdot f_z \tag{4}$$

where τ_θ is the torque in the θ domain, f_z is the force in the z domain and $\frac{dz}{d\theta}$ is the slope of the NTF characteristic.

At either end of the stroke, the slope of the NTF characteristic, $\frac{dz}{d\theta}$, is very small. Thus, the reflected motor inertia in the z domain is very large, creating inherently smooth valve kinematics profiles, since the valve is slowed down by the large effective inertia when it is opened and closed. Moreover, the large spring force at the ends of the stroke when reflected to the θ domain is small, allowing the use of small motor currents to hold the valve open or closed. In effect, the NTF enables the use of small holding and driving currents when actuating the valve. In addition, because the gas force on the exhaust valve is largest at the opening end of the exhaust stroke, the reflected gas force in the θ domain is also small. This characteristic makes it easy to open the valves against a large gas force. Thus, the proposed EMVD allows for the use of motors with small size.

IV. Controller Design and Simulation

The equations of motion for the proposed EMVD shown in Fig. 6 are as follows [8]:

$$f_z = m_v \cdot \frac{d^2z}{dt^2} + b_v \cdot \frac{dz}{dt} + K \cdot z \tag{5}$$

$$J \cdot \frac{d^2\theta}{dt^2} + b \cdot \frac{d\theta}{dt} + \tau_\theta = K_T \cdot i \tag{6}$$

where τ_θ is torque in the θ domain, f_z is the force in the z domain, J is the inertia in the θ domain, m_v is the mass in the z domain, b is the friction in the θ domain, b_v is the friction in the z domain, K_T is the motor torque constant, K is the spring constant, θ is the displacement in the rotational domain, and z is the displacement in the vertical domain.

Equations (5) and (6) can be combined using the NTF characteristic (1), (2), (3), and (4). In this manner, we can obtain a single equation of motion in either the z or the θ domains. This equation will be nonlinear, since linear equations such as (5) and (6) are transformed to nonlinear equations in the other domain because of the NTF characteristic. Moreover, we can write state equations for the EMVD in either the z or the θ domains. Denoting position and velocity in the z domain by x_1 and x_2 respectively, the following nonlinear state equations are obtained in the z domain.

$$\dot{x}_1 = x_2 \tag{7}$$

$$\dot{x}_2 = F_1(x_1, x_2) + F_2(x_1, x_2) \cdot i \tag{8}$$

where i is the control input (motor current) and

$$F_1(x_1, x_2) = \frac{-\{(b_v + b \cdot (\frac{d\theta}{dz})^2) \cdot x_2 + J \cdot \frac{d^2\theta}{dz^2} \cdot \frac{d\theta}{dz} \cdot x_2^2 + K \cdot x_1\}}{m_v + J \cdot (\frac{d\theta}{dz})^2} \tag{9}$$

$$F_2(x_1, x_2) = \frac{\frac{d\theta}{dz} \cdot K_T}{m_v + J \cdot (\frac{d\theta}{dz})^2} \tag{10}$$

A block diagram of the feedback-controlled EMVD apparatus is shown in Fig. 8. The reference input is the desired valve position, and the system output is the actual valve position. The difference between the two is passed into a controller which provides an appropriate current input to a motor drive. This motor drive supplies the desired current to the motor. Note that, for simplicity, this model assumes a perfectly responding motor drive which supplies as much current to the motor as desired, and assumes nothing about the dynamics of the motor drive.

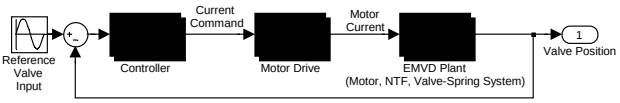

Fig. 8. The EMVD as a Feedback Control System.

The maximum valve transition times required at engine speeds of 6000rpm are approximately 3-4ms. Based on these transition times, the required natural frequency of the proposed EMVD is approximately 150Hz, which is approximately the reciprocal of twice the required valve transition time. Thus, the feedback-controlled EMVD must be able to respond to inputs with frequencies of approximately 150Hz. Considering this fact, we decided on an overall control system bandwidth of approximately 1kHz. This bandwidth in turn constrains the bandwidth of the position sensors and the motor drive to be approximately 10kHz, as it is desirable for the sensor dynamics not to affect the feedback-controlled EMVD dynamics.

There are several issues that must be considered when designing controllers for the proposed EMVD. First, it is important to note that the dynamic characteristics of the proposed EMVD change along the valve stroke. At the ends of the stroke,

the effective inertia in the z domain is large, while at the midpoint of the stroke, this effective inertia is small. Thus, in the z domain, the effective system gain of the valve-spring system decreases at the ends of the stroke and increases at the midpoint of the stroke.

A linear control law, such as a fixed-gain proportional-plus-derivative (PD) controller, is not well-suited to the control of this EMVD. Such a control law can work well only if the PD controller gains are varied with valve position [8]. In this respect, one possible control technique that can be implemented is that of piecewise linearization. In this technique, the state space is divided into sections where the nonlinear system is approximately linear and a different control law is used to govern the motion when the system is in a particular region of the state space [20]. When applied to the proposed EMVD, this technique corresponds to dividing the z domain into regions such that the slope of the NTF characteristic (in Fig. 7) is approximately linear in each region. An appropriate controller can then be used to control the system in each region.

An alternative to the piecewise linearization technique is to use a nonlinear gain-varying function. In this method, a nonlinear mapping is used such that the controller gains are varied as the system moves from operating in one part of the state space to another. Such nonlinear controllers are easily implemented [21], [22].

Another common control method is that of designing a nonlinear controller which takes into account the nonlinear system dynamics of the plant. An example of such a controller is one based on feedback linearization [20]. The control law for a feedback-linearized nonlinear controller for the proposed EMVD is:

$$i = \frac{\ddot{x}_{1,d} - F_1(x_1, x_2) - k_0 \cdot (x_1 - x_{1,d}) - k_1 \cdot (\dot{x}_1 - \dot{x}_{1,d})}{F_2(x_1, x_2)} \tag{11}$$

where $x_{1,d}$ is the desired valve position, and k_0 and k_1 are appropriate controller gains [8]. These gains can be determined such that the closed-loop system has a 1kHz bandwidth.

The NTF characteristic we chose is almost flat at the ends of the stroke (when $z \rightarrow \pm 4$mm in Fig. 7). This characteristic deteriorates the valve transition time for the EMVD because the acceleration of the valve when it is near the end of the stroke is small. In order to solve this problem, a feedforward control technique can be used: pulses of current can be applied to the motor when the valve is near either end of the stroke. This current injection technique results in an almost 50% reduction in the transition time of the valve when compared to simulations where the technique is not used [8].

Fig. 9 shows results from a MATLAB simulation of the proposed EMVD, including the effects of gas force, friction and electric motor losses, using reasonable electrical and mechanical parameters [8]. A variety of control laws were used in this simulation. At the beginning of the simulation, a combination of current injection and a PD controller were used. After the brief period of current injection, the feedback linearization-based control law in (11) was used. In addition, during the holding time period, another PD controller was used. The spikes in seen in Fig. 9 are because of switching the control laws, and can be eliminated in practice [4].

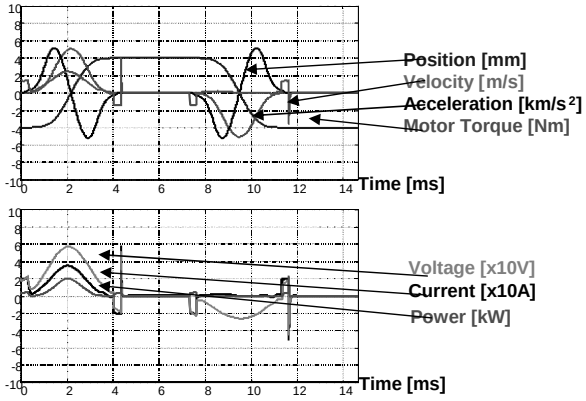

Fig. 9. Simulation of the MIT Electromagnetic Valve Drive.

The simulation results show significant improvements over normal-force actuated valve-spring systems and bi-directional shear-force actuated valve-spring systems without a NTF. The holding and driving currents are small, and the overall power appears to be technically and economically feasible. In the simulation, which was carried out at 6000rpm engine speed (corresponding to fast transition times) and wide open throttle conditions, the transition time for the valve was approximately 4ms, the seating velocity was less than 0.5cm/s. The total average electrical power input was approximately 1.2kW for 16 valve actuators in a 2.0L, 4-cylinder engine. In comparison, the average power for a conventional IC engine is 3kW, while that for a IC engine with roller-follower type cams is 1.5kW [8]. These power losses include both the required power to compensate for gas forces and the electrical and mechanical power losses in the EMVD.

V. The Experimental EMVD Apparatus

In order to prove the concept of the proposed EMVD, we have designed and constructed an experimental apparatus on a workbench. This section describes some of the design challenges for the experimental apparatus.

The mechanical components for the EMVD apparatus were designed in 3-dimensional solid modeling software. The mass and inertia of the mechanical components of the EMVD apparatus was our primary concern. The larger the mass/inertia

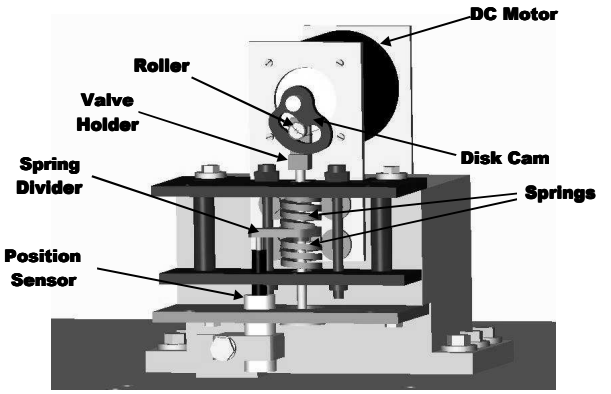

Fig. 10. Cross-Section of the Experimental Apparatus modeled in SolidWorks.

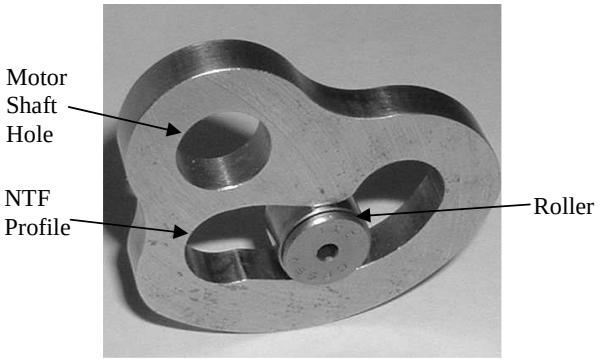

Fig. 11. The Nonlinear Mechanical Transformer - Disk Cam.

of components in the system, the larger the strain on the motor. Thus, we tried to make the components as small and light as possible without compromising their mechanical capabilities. Fig. 10 shows a cross-sectional-view of the 3-dimensional model that was put together in 3-dimensional solid modeling software.

To meet the 150Hz natural frequency requirement of the proposed EMVD, we chose springs with the appropriate z domain stiffness and effective inertia characteristics. Effective inertia comprises the total mass in the z domain and the mass from the θ domain reflected to the z domain through the NTF characteristic equations (1), (2), (3), and (4). The stiffness of the springs was determined after carefully choosing an appropriate modulus for the NTF. It is important to note that the inertia of the springs and the NTF cannot be neglected because they have a strong affect on system dynamics.

For simplicity, we chose a disk cam to be the NTF. The motor shaft is rigidly connected to the disk cam having a shaped slot as shown in Fig. 10. As the disk cam rotates with the motor shaft, a roller whose shaft is connected to the valve rolls over either the top or the bottom surface of the slot of the disk cam. The valve and the shaft of the roller are free to move up and down but constrained from other motions. The shape of the slot can determine a desired nonlinear mechanical transformer characteristic, such as that in Fig. 7. An appropriate linearized modulus of the NTF was chosen so that the maximum available power in the θ domain could be delivered to the load in the z domain. In order to obtain this maximum power transfer, the mid-stroke transformer modulus was chosen so that the reflected inertia from the θ domain was matched with the mass in z domain. Fig. 11 shows a picture of the constructed disk cam.

Standard exhaust engine valves from a Ford ZETEC 2.0L cylinder head were used in the proposed EMVD apparatus. The masses of the valves were determined to be similar to values used in simulations. We may consider using ultra-light engine valves (Eaton Corporation's ULVs) in later versions of our experimental apparatus.

We obtained an off-the-shelf motor (Pacific Scientific's 4N63) with a large torque/rotor inertia ratio, high power rating, and appropriate electrical and mechanical time constants for the proposed EMVD. In particular, we chose a motor with low inductance (100μH) and low resistance (1Ω) in order to make it easier to meet the slew rate requirement on the motor drive. The motor was also chosen because it is able to respond with enough torque up to frequencies of 150Hz, and has an appropriate K_T. The adequacy of these motor characteristics was determined using simulation results from the previous section. Unfortunately, the motor we chose was large in size – too large to be easily implemented in an actuation system on a engine head. Nonetheless, we selected an off-the-shelf motor because a custom-made motor would have been much smaller in size but much more expensive. When the proposed EMVD is implemented on a cylinder head, smaller motors will have to be obtained.

Bearing in mind the bandwidth and power constraints mentioned above, as well as the mass/inertia and size constraints, we obtained several other components for the EMVD apparatus, including a linear position sensor (Sentech's Fastar FS300), a rotary optical encoder (US Digital's E6D), a PC, and a digital signal processing board (dSPACE's DS 1104). We planned to used the PC and DS1104 board to implement controllers for the proposed EMVD. Wherever possible, we selected off-the-shelf components.

The rotary optical encoder chosen has a 2048-line resolution. This number of lines gives high enough resolution and bandwidth for our application. In particular, the reflected resolution of the sensor, when viewed from z domain becomes higher as the valve approaches an end of the stroke. From a control point of view, this high resolution implies that high precision position control can be carried out at the ends of the stroke, where the valve's seating velocity must be effectively controlled. We also chose a high-bandwidth, low mass, variable-reluctance type linear position sensor. This sensor, although not critical to the con-

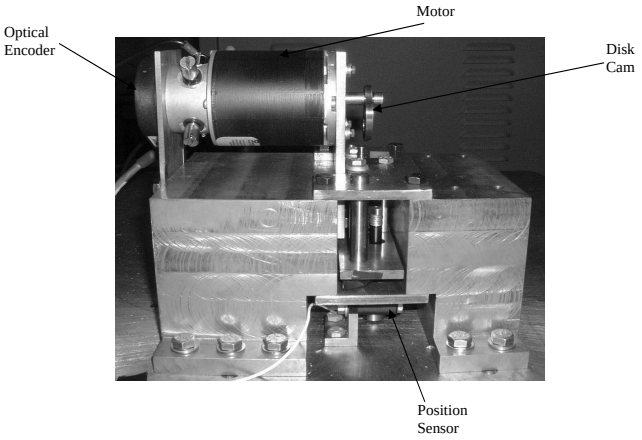

Fig. 12. Picture of the Assembled EMVD Apparatus.

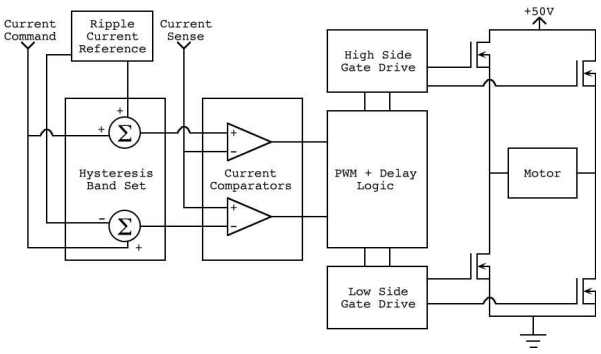

Fig. 13. A Hysteretic Current-Controlled Motor Drive.

trol of the EMVD, allows for an investigation of the effects of the compliance between the motor and the valve.

Fig. 12 shows a picture of the assembled bench-top EMVD apparatus. Motor and valve displacements from the EMVD apparatus are sensed by ADC channels on the dSPACE board. A controller that is modeled in MATLAB's Simulink software on the PC and implemented on the dSPACE board, provides a control input to the motor drive circuit via a DAC channel. This control input is calculated using the measured displacement and the displacement command function. We used a 50kHz sampling frequency for the DAC and ADC channels on the dSPACE board.

VI. Implications for the Electrical/Electronic Components

The proposed EMVD poses significant challenges in the area of electrical/electronic component design. In addition to the constraints set on the selection of appropriate sensors for the EMVD apparatus, there are several constraints on the power electronics required to drive the motor.

The simulation of Fig. 9 assumed that a high-bandwidth current source was instantaneously supplying current to the motor. Because it was not possible to obtain a high-bandwidth motor drive for the EMVD apparatus at a reasonable cost, we had to design and construct an appropriate motor drive.

There were three primary design constraints on the motor drive: because of the use of the current injection technique to control the EMVD, we needed a motor drive with a high slew rate (70A/ms) capability; the bandwidth of the motor drive had to be approximately 10kHz; and finally, the motor drive had to be able to source approximately 1kW of average power.

We selected a current-control input for the feedback-controlled EMVD system. This method provides a direct relationship between input signal and motor torque, with fast response to changes in the desired valve profile. We chose a full-bridge inverter topology with hysteretic current control to implement the motor drive circuit [23], [24]. A block diagram of the hysteretic current-controlled full-bridge motor drive circuit with a 50V bus voltage is shown in Fig. 13. Hysteresis current control keeps the actual motor current within a certain hysteresis band of the desired motor current by switching on opposite pairs (a high-side MOSFET on one side of the bridge and a low-side MOSFET on the other side of the bridge) of MOSFETs in the bridge. This control method features a simple control loop, fast response time and well-defined ripple current. However, due to the non-integrating nature of the feedback loop, the controller has a non-zero tracking error. In addition, the switching frequency varies as a function of load and input signal.

The slew rate of the amplifier determines how fast large amounts of current can be driven into the load. A slew rate of 70A/ms was determined to be optimal based on current waveforms in simulations where we used the current injection technique. A higher slew rate makes the ripple current higher for fixed switching frequencies, or increases the switching frequency for fixed ripple current. The hysteretic current-control design is highly sensitive to the applied load – in this case, the resistance and inductance of the motor in series with the motor's back EMF. Solving Kirchoff's voltage law for this load yields:

$$V_{bus} = i \cdot R + K_{emf} \cdot \omega + L \cdot \frac{di}{dt} \tag{12}$$

The control circuit on the motor drive was designed for an EMVD apparatus without gas force disturbances. With no gas force, the maximum driving current condition (for maximum acceleration) occurs when the angular velocity is approximately zero. Similarly, the required current at maximum velocity is low (unless the effects of gas force are added). The motor has an inductance of 100μH, an armature resistance of 1Ω and a back EMF constant of 7.33V/kRPM. From simulations of the feedback-controlled EMVD (see Fig. 9), a maximum required slew rate of approximately 40A/ms was calculated, including

the effects of gas force. To leave some margins on the slew rate, we decided to design the motor drive to have a 70A/ms slew rate. Note that with a 14V bus voltage, it would not have been possible to achieve a 70A/ms slew rate.

The hysteresis band, ripple current, and switching frequency are related by (13). These quantities were determined after selecting the appropriate bus voltage and slew rate. The hysteresis band was chosen to obtain a reasonable ripple current at a switching frequency that does not dissipate too much power. Although the hysteretic current-control method does not have a fixed frequency, a worst-case frequency can be found for a particular hysteresis band. Assuming a worst-case frequency of 300kHz, we chose the IR2807 MOSFET (in a TO-220 package) to minimize the power dissipation. At a load current of 15A, switching frequency of 300kHz, and ripple current of 0.95A, a MOSFET at nearly 100% duty cycle would have a switching loss of 3.09W and a conduction loss of 5.35W, totalling 8.44W for each of four MOSFETS in the bridge.

$$I_{ripple} = \frac{1}{2} \cdot T \cdot \frac{di}{dt} = \frac{1}{2f} \cdot \frac{V_{BUS}}{L} \tag{13}$$

A working model of the motor drive inverter circuit was constructed. A photograph of the completed motor drive circuit appears in Fig. 14. A few design parameters, together with the values actually achieved are shown in Table I. In the motor drive tests, the thermal performance of the amplifier was observed to be empirically superior to that expected when the circuit was designed.

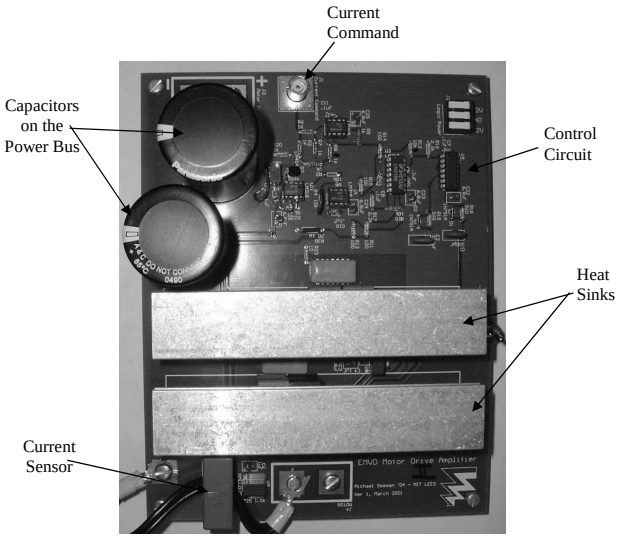

Fig. 14. The Motor Drive Inverter Circuit.

Fig. 15 shows a Simulink model of the hysteric current-controlled motor drive with the selected motor. The 42V bus voltage and approximately 2A peak-to-peak ripple current specified the hysteresis block in this model. The electromechanical dynamics of the motor are included in the model.

Quantity	Desired Value	Measured Value
Slew Rate	70A/ms	69A/ms
Bandwidth	10kHz	9.5kHz
Power	1kW	$\geq$ 1kW
Current Ripple	$\leq$ 1A	0.98A

TABLE I
CHARACTERISTICS OF THE MOTOR DRIVE.

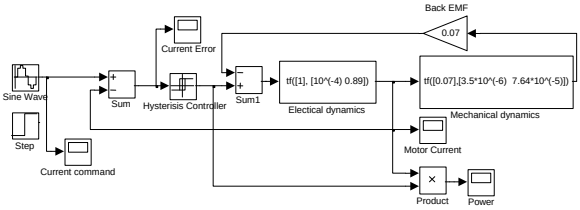

Fig. 15. Simulink Model of a Hysteretic Current-Controlled Motor Drive.

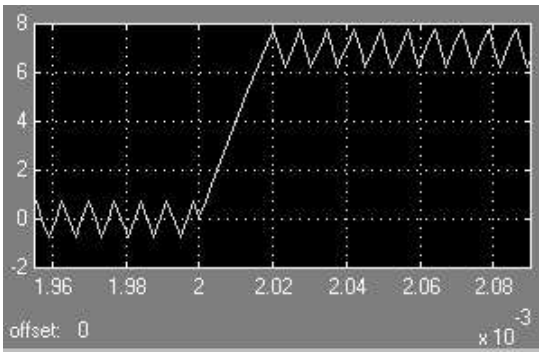

Fig. 16. Simulated Step Response of the Motor Drive/Motor Combination with a 7A step input.

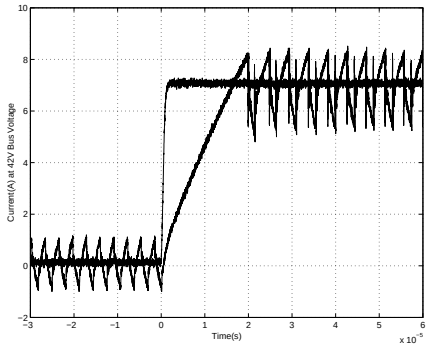

Fig. 17. Step Response of the Motor Drive/Motor Combination with a 7A step input.

Figs. 16 and 18 show simulation results for the step response

of the motor drive/motor combination with a 7A step input, and the time response of the motor drive/motor combination with a 7A, 3kHz sinusoidal current command, respectively. Figs. 17 and 19 show experiment results for the same reference inputs and bus voltage as in the simulations. From these figures, we see that the experimental results agree with the simulations.

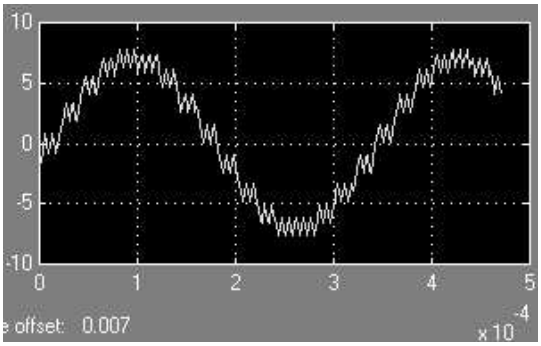

Fig. 18. Simulated Output Current Waveform for the Motor Drive with a 7A, 3kHz sinusoidal current command.

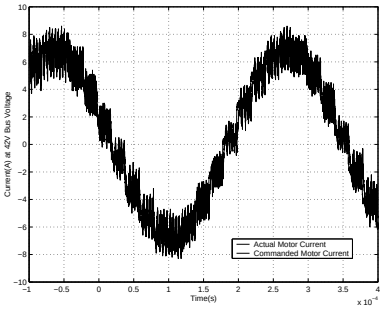

Fig. 19. Input/Output Current Waveform for the Motor Drive with a 7A, 3kHz sinusoidal current command.

VII. Conclusion

We recently proposed an EMVD for actuating internal combustion engine valves [8]. This paper summarized previous work in the area of electromagnetically actuated VVT systems, and explained the operation of the proposed EMVD. In addition, some design issues for a bench-top experimental EMVD apparatus we have constructed have been addressed. The proposed EMVD design has several implications for the required electrical/electronic components for the EMVD apparatus. Future research work includes further testing of the EMVD apparatus, confirmation of the benefit of the nonlinear mechanical transformer, and the design of more optimal controllers for the system, including but not limited to controllers that will minimize the power consumption of the system.

Acknowledgments

We would like to thank Ford Motor Company and Eaton Corporation for the donation of two engine heads. We also thank Mr. George Yundt from Danaher Motion Corporation, Dr. David Turner from Eaton Corporation, and Dr. Bruno Lesquesne from Delphi Automotive Systems for their advice.

References

[1] J. G. Kassakian, H-C. Wolf, J. M. Miller, and C. J. Hurton, "Automotive Electrical Systems Circa 2005," *IEEE Spectrum*, pp. 22–27, August 1996.

[2] J. G. Kassakian, H-C. Wolf, J. M. Miller, and C. J. Hurton, "The Future of Automotive Electrical Systems," in *IEEE Workshop on Power Electronics in Transportation*, pp. 3–12, Dearborn, MI, October 24-25, 1996.

[3] J. G. Kassakian, "The Role of Power Electronics in Future 42V Automotive Electrical Systems," in *EPE-PECM Conference*, pp. 3–11, Dubrovnik, Croatia, Sept. 2002.

[4] W. S. Chang, *An Electromechanical Valve Drive Incorporating a Nonlinear Mechanical Transformer*. Ph.D. thesis proposal, Massachusetts Institute of Technology, 2001, unpublished.

[5] M. B. Levin, and M. M. Schlecter, "Camless Engine," *SAE Technical Paper Series*, Paper 960581, 1996.

[6] P. Barkan, and T. Dresner, "A Review of Variable Valve Timing Benefits and Modes of Operation," *SAE Technical Paper Series*, Paper 891676, 1989.

[7] T. Ahmad, and M. A. Theobald, "A Survey of Variable-Valve-Actuation Technology," *SAE Technical Paper Series*, Paper 891674, 1989.

[8] W. S. Chang, T. A. Parlikar, J. G. Kassakian, and T. A. Keim, "An Electromechanical Valve Drive Incorporating a Nonlinear Mechanical Transformer," in *SAE World Congress*, Detroit, MI, March 2003, in press.

[9] F. Pischinger *et al.*, "Electromechanical Variable Valve Timing," *Automotive Engineering International*, 1999.

[10] F. Pischinger *et al.*, "Arrangement for Electromagnetically Operated Actuators," *US Patent #4,515,343*, 1985.

[11] "Camless BMW Engine Still Faces Hurdles," *Automotive Industries*, pp. 34, October 1999.

[12] R. Flierl, and M. Klüting, "The Third Generation of Valvetrains – New Fully Variable Valvetrains for Throttle-Free Load Control," *SAE Technical Paper Series*, Paper 2000-01-1227, 2000.

[13] M. A. Theobald, B. Lesquesne, and R. R. Henry, "Control of Engine Load via Electromagnetic Valve Actuators," *SAE Technical Paper Series*, Paper 940816, 1994.

[14] "Renault Research," *Automotive Engineering International*, pp. 114, March 2000.

[15] "Emission Control," *Automotive World*, pp. 10–15, April 2000.

[16] S. Butzmann, *et al.*, "Sensorless Control of Electromagnetic Actuators for Variable Valve Train," *SAE Technical Paper Series*, Paper 2000-01-1225, 2000.

[17] M. Gottschalk, "Electromagnetic Valve Actuator Drives Variable Valvetrain," *Design News*, November 1993.

[18] R. R. Henry, and B. Lesquesne, "A Novel, Fully-Flexible, Electromechanical Engine Valve Actuation System," *SAE Technical Paper Series*, Paper 970249, 1997.

[19] R. R. Henry, and B. Lesquesne, "Single-cylinder Tests of a Motor-driven, Variable-valve Actuator," *SAE Technical Paper Series*, Paper 2001-01-0241, 2001.

[20] J-J. Slotine, and W. Li, *Applied Nonlinear Control* Prentice-Hall, 1991.

[21] M. F. Schlecht, "Time-Varying Feedback Gains for Power Circuits with Active Waveshaping," in *IEEE Power Electronics Specialists Conference*, pp. 15–22, July 1981.

[22] A. M. Stankovic, D. J. Perreault, and K. Sato, "Synthesis of Dissipative Nonlinear Controllers for Series Resonant DC/DC Converters," *IEEE Transactions on Power Electronics*, Vol. 14, No. 4, pp. 673–682, July 1999.

[23] A. B. Plunkett, "A Current-Controlled PWM Transistor Inverter Drive," *IEEE/IAS Annual Meeting Conference Record*, pp. 789–792, 1979.

[24] D. M. Brod, and D. W Novotny, "Current Control of VSI-PWM Inverters," *IEEE Transactions on Industrial Applications*, Vol. IA-21, No. 4, pp. 562–570, June 1985.